Study of Dielectric and Magnetoelectric Properties of $Cu_{0.8}Co_{0.2}Fe_2O_4$: $PbZr_{0.58}Ti_{0.42}O_3$ Particulate and Laminated Film Composites

Bhavana H.V, Shaik Sabira Begum, S.S. Bellad*
Department of Physics, Materials Research Center,
Maharani Science College for Women, Bengaluru -560 001
*Author for correspondence: (ssbellad@rediffmail.com)

Abstract: The solid-state reaction approach is used to produce magnetoelectric composites having ferrite phase $Cu_{0.8}Co_{0.2}Fe_2O_4$ and ferroelectric phase $PbZr_{0.58}Ti_{0.42}O_3$ (PZT). The hydraulic pressing method is used to make particulate composites of $yCu_{0.8}Co_{0.2}Fe_2O_4$-(1-y) PZT and the screen printing technique is used to make laminated thick films of $Cu_{0.8}Co_{0.2}Fe_2O_4$/PZT/ $Cu_{0.8}Co_{0.2}Fe_2O_4$. The existence of cubic spinel structure in the ferrite phase and tetragonal perovskite structure in the ferroelectric phase is revealed by XRD. Detailed analysis of dielectric properties was done under the idea that magnetoelectric interactions between constituent ferrite and ferroelectric phases could result in unique anomalies in dielectric behaviour of both particulate composites and laminated thick film composites. The variation of dielectric constant and loss tangent with frequency and temperature for both particulate and laminated thick film composites was investigated and explained using the phenomenon of space charge polarisation. AC resistivity with frequency exhibits the same behaviour for both composites i.e., as frequency increases, resistivity reduces and vice versa and is explained by charge carrier hopping between distinct ionic sites. DC resistivity measurements exhibit semiconducting nature for both composites. The magnetoelectric conversion factor $(ME)_H$ was investigated as a function of the DC magnetic field for both particulate composites and laminated thick films. For laminated thick film composites of $Cu_{0.8}Co_{0.2}Fe_2O_4$/PZT/$Cu_{0.8}Co_{0.2}Fe_2O_4$, magnetoelectric coefficient of about 69 mv/OeCm is observed, while magnetoelectric coefficients of about 90 mv/OeCm, 77 mv/OeCm, and 53 mv/OeCm are observed for particulate composites of $y(Cu_{0.8}Co_{0.2}Fe_2O_4) + (1-y)PbZr_{0.58}Ti_{0.42}O_3$ where y= 0.25, 0.5, 0.75.

Keywords: ME composites, Ferrites, Ferroelectrics, screen printing, ME effect

1. Introduction

Multiferroic composites are the new class of multifunctional materials that have received a lot of attention in recent years because of their potential applications in memory devices, sensors, magnetic refrigeration, microwave devices, energy harvesters, and conversion devices [1-3]. These composites are created by combining two or more single-phase compounds and the physical properties of these composites are determined by the properties of their constituent phases and their interaction [4]. However, the magnetoelectric effect (ME) is a significant property of multiferroic composites that is observed due to polarization-magnetization coupling. In a brief description, when a magnetic field is applied to the composites, magnetic phase magnetostrictively changes its shape. The strain generated is then transferred to the piezoelectric phase, resulting in electric polarisation [5]. As a result, materials with high magnetostriction and piezoelectric coefficient are required to create composites with high magnetoelectric (ME) output. There are two types of multiferroic materials: single phase and composites. Single-phase multiferroics have poor ME coupling, limiting their use in devices. The composite materials are the better alternative to these materials because high ME coupling can be realized in these materials by combining good quality piezoelectric and magnetostrictive phases [6]. Van Suchetelen[7] defined the product property of magnetoelectric composites as a suitable combination of magnetostrictive and piezoelectric phases [7]. Particulate ME composites and laminated film ME composites have gained prominence in recent years because of their applications in innovative

technologies. Above room temperature, bulk/ particulate ME composites exhibit a strain-mediated ME effect and laminated films produce a reduction in a loss at the interface due to the atomic level combination of different phases. As a result, particulate ME composites and laminated ME films are more promising candidates for use in spintronics, magnetic field sensing devices, high-power transmission system current measurement, microwave ovens as leak detectors, switching devices, integral optics, fibre communication technology, and other multifunctional devices [8-10]. As an outcome, many researchers have studied the electrical and magnetoelectric properties of particulate ME composites and laminated ME films such as $(1-x)BaTiO_3$-$xCoFe_2O_4$[11], $Ba_{0.95}Ca_{0.05}Ti_{0.90}Zr_{0.10}O_3$-$La_{0.67}Sr_{0.33}MnO_3$[12], $Ba_{0.5}Sr_{0.5}Nb_2O_6/CoCr_{0.4}Fe_{1.6}O_4$[13], $(1-x)Na_{0.5}Bi_{0.5}TiO_3$-$(x)CoCr_{0.4}Fe_{1.6}O_4$ [14], (1-x)BCZT-xCFO [15], $(1-x)\ PbZr_{0.55}Ti_{0.45}O_3 + (x)\ Co_{0.8}Ni_{0.2}Fe_2O_4$ [16], $BaTiO_3/NiFe_2O_4$ [17], PFW-PT [18], Fe-Ga/$Pb(Mg_{1/3}Nb_{2/3})O_3$-$PbTiO_3$ [19], etc .

Lead zirconium titanate is the most widely utilized ferroelectric material due to its high resistivity and dielectric permittivity. It has also been shown to have exceptional piezoelectric and electromechanical properties for composites close to the Morphotropic Phase Boundary region (i.e., x = 0.52-0.6) [20]. Vijendra et al. [21] used solid-state reaction approach to create $PbZr_xTi_{1-x}O_3$ ($0.0 \leq x \leq 1.0$) ceramics and discovered that as Zr content increased, activation energy values decrease. S.P. Yadav et al. [22] synthesized PZT and reported room temperature dc resistivity of about $1.146x10^5(\Omega.cm)$, saturation polarisation (5.60, 4.93 and 3.19C/cm^2) and remanence polarisation (4.53, 2.23 and 1.28C/cm^2) was observed at 100°C, 150°C and 200°C respectively. Copper-cobalt ferrite ($CuCoFe_2O_4$) is used as a ferromagnetic material because it has high magnetostriction compared to all other ferrites. Jnaneshwara et al. [23] produced $Co_{1-x}Cu_xFe_2O_4$ and demonstrated that as Cu^{2+} concentration increased, saturation magnetization reduced from 38.5 to 26.7 emu g^{-1}. Jonker [24] investigated the electrical properties of bulk $Co_{3-X}Fe_XO_4$ ferrites and discovered that hole hopping between Co^{2+} and Co^{3+} ions contribute to low conductivity regions whereas hopping between Fe^{2+} and Fe^{3+} ions contribute to high conductivity regions. Electrical and magnetoelectric properties for particulate ME composites and laminated thick film ME composites have not been reported in the literature, so dielectric properties, resistivity measurements, and magnetoelectric properties are investigated in this research paper by using ferrite phase $Cu_{0.8}Co_{0.2}Fe_2O_4$ and ferroelectric phase $PbZr_{0.58}Ti_{0.42}O_3$.

2. Experimental details

Synthesis of Particulate composites:

Using a solid-state reaction technique, magnetoelectric composites with ferrite phases $Cu_{0.8}Co_{0.2}Fe_2O_4$ and $PbZr_{0.58}Ti_{0.42}O_3$ are produced. For the synthesis of ferrite phase, starting materials such as powders of CuO, Co_3O_4 and Fe_2O_3 are used, while powders of PbO, ZrO_2, and TiO_2 are used to prepare the ferroelectric phase. These oxides are weighed stoichiometrically and mixed in an agate mortar with acetone as a medium. Since the metal oxide reactions cannot occur at room temperature, they are kept for pre-sintering which is carried out separately at 600^{0}C and 650^{0}C for about 6 hours. To create particulate composites with compositions $y(Cu_{0.8}Co_{0.2}Fe_2O_4)+(1-y)\ PbZr_{0.58}Ti_{0.42}O_3$, where y= 0.25, 0.5 and 0.75, the mixture of ferrite and ferroelectric powders must first be mixed with a 10% PVA solution, pressed into pellet form and then subjected to the final sintering process at 900^{0}C for about 12 hours.

Synthesis of laminated thick film composites:

Magnetoelectric composites with ferrite phases $Cu_{0.8}Co_{0.2}Fe_2O_4$ and $PbZr_{0.58}Ti_{0.42}O_3$ are synthesized using a solid-state reaction technique. Powders of CuO, Co_3O_4 and Fe_2O_3 are used as starting materials for the synthesis of ferrite phase, while PbO, ZrO_2, and TiO_2 are used to prepare ferroelectric phase. These oxides are weighed stoichiometrically and combined with acetone as a medium in an agate mortar. Since metal oxide reactions cannot take place at room temperature, they are kept for pre-sintering which is done separately for about 6 hours at 600^{0}C and 650^{0}C. For the production of thick laminate films $Cu_{0.8}Co_{0.2}Fe_2O_4$ /PZT/ $Cu_{0.8}Co_{0.2}Fe_2O_4$, screen-

printing method is used which is very simple, economical method for deposition of thick films. A paste of ferrite and ferroelectric powders is prepared by mixing powder with a 10% ethyl cellulose solution which is made by combining binder ethyl cellulose with solvent terpineol. The prepared paste is then squeezed on the mesh so that it spreads paste onto FTO substrate. In order to deposit thick films, first ferrite layer must be deposited on the FTO substrate and dried at room temperature for 12 hours. Then, the second layer, PZT, must be deposited on the ferrite layer and dried in a manner similar to that of the first layer. The third layer i.e ferrite layer is then deposited and left to dry. Thus, final sintering is carried out at 300^0 C for 30 minutes following fabrication of laminated thick film composites of $Cu_{0.8}Co_{0.2}Fe_2O_4$/ PZT/ $Cu_{0.8}Co_{0.2}Fe_2O_4$. The formation of laminated thick film composites is shown in Figure 1.

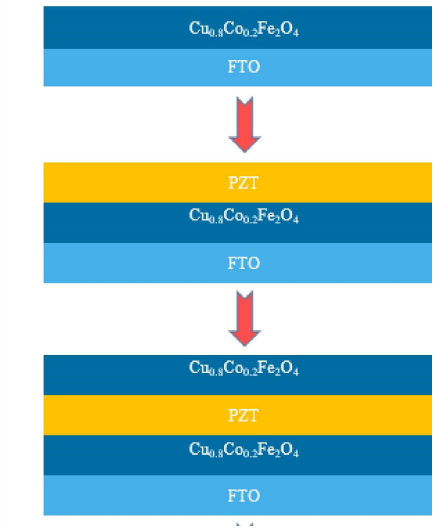


Figure 1: Fabrication of laminated thick film composites

3. Results and Discussions

Figures 2 and 3 provide representative XRD for ferrite phase $Cu_{0.8}Co_{0.2}Fe_2O_4$ and ferroelectric phase PZT. According to XRD, ferrite phase has a cubic spinel structure with peak (311) as the dominant peak, whereas ferroelectric phase has a tetragonal perovskite structure with peak (101) representing as the high intensity peak [25].

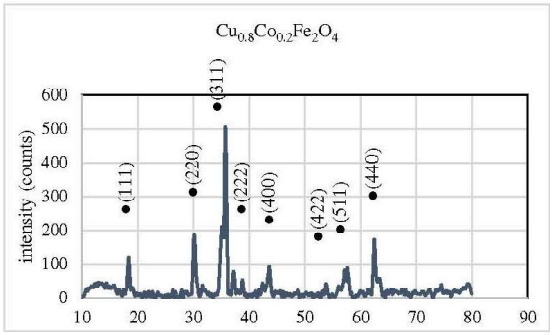


Figure 2: Typical XRD pattern of $Cu_{0.8}Co_{0.2}Fe_2O_4$

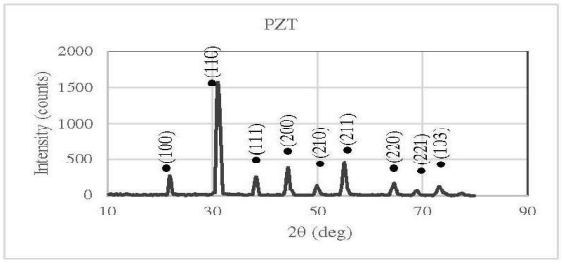


Figure 3: XRD pattern of PZT

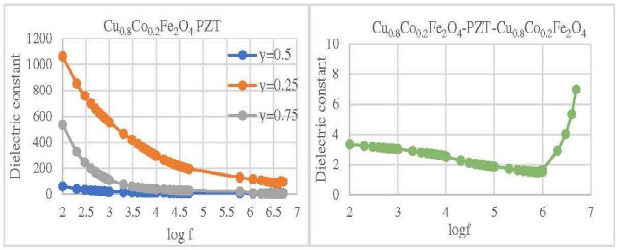


Figure 4 : Variation of dielectric constant with frequency for particulate ME composite $yCu_{0.8}Co_{0.2}Fe_2O_4$-(1-y)PZT and laminated tri-layered thick films ($Cu_{0.8}Co_{0.2}Fe_2O_4$/ PZT/ $Cu_{0.8}Co_{0.2}Fe_2O_4$) measured at room temperature.

Using the impedance analyser Wayne Kerr 6500, the electrical properties of particulate composites and laminated thick film ME composites were investigated. Figure 4 depicts the variation of dielectric constant with frequency for both composites at room temperature which is explained by the space charge polarization/interfacial polarisation described by Maxwell Wagner's interfacial theory which is consistent with Koop's phenomenological theory [26]. From Figure 4 it is seen that dielectric constant of particulate composites decreases rapidly with increasing frequency and reaches saturation at higher frequencies with dielectric constants of about 1060, 61.4 and 536 observed for y= 0.25, 0.5, and 0.75 at low frequency respectively. The dielectric constant of laminated thick film composites decreases

up to 1MHz and increases above that frequency with a dielectric constant of around 3.35 observed at low frequency. Dielectric dispersion at low frequencies are attributed to space charge polarisation and valence state of cations like Fe^{3+}/Fe^{2+}, Co^{2+}/Co^{3+}, Cu^{2+}/Cu^{1+}. At low frequencies, polarization is produced by the exchange of electrons between cations [27]. The inhomogeneous dielectric structure in composite materials causes dielectric dispersion which is affected by porosity, grain size, and impurities [27].

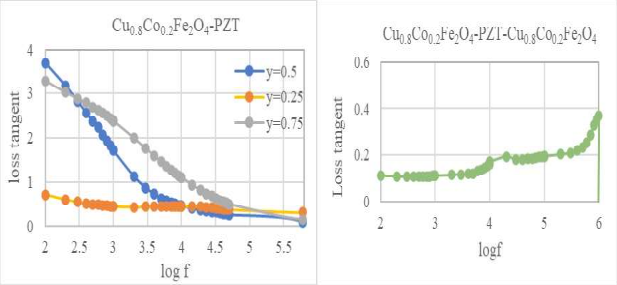


Figure 5 : Variation of loss tangent with frequency for particulate ME composite $yCu_{0.8}Co_{0.2}Fe_2O_4$-(1-y)PZT and laminated tri-layered thick film ($Cu_{0.8}Co_{0.2}Fe_2O_4$/PZT/ $Cu_{0.8}Co_{0.2}Fe_2O_4$) measured at room temperature.

Figure 5 depicts the frequency dependence of loss tangent for particulate and laminated thick film composites. Loss tangent for $yCu_{0.8}Co_{0.2}Fe_2O_4$-(1-y) PZT particulate composites follows the same trend as dielectric constant with frequency and is found to be 3.29, 3.7, 0.71 for y= 0.25, 0.5, 0.75 respectively. For laminated film composites of $Cu_{0.8}Co_{0.2}Fe_2O_4$/ PZT/ $Cu_{0.8}Co_{0.2}Fe_2O_4$, with the increase in frequency loss tangent slightly decreases up to 1kHz and increases slightly above that frequency and at low-frequency, loss tangent is found to be 0.11. At low frequencies, charge carrier accumulation at the interface is greater in composites resulting in more dissipation or losses. However as frequency increases, charge carrier accumulation decreases and loss tangent decreases [27]. The temperature dependence of dielectric constant for particulate composites and laminated thick films is shown in Figure 6. In case of particulate composites, it is noted that the dielectric constant exhibits absorption peaks at 553K and 503K for y=0.5 and 0.75, respectively which correspond to the curie temperature, with the exception of y=0.25 composites where dielectric constant increases as the temperature rises. For the laminated thick films, dielectric constant is constant up to 400^0 K and increases with temperature above that point. Below 400^0 K, dielectric constant exhibits flatness because hopping of the electrons in these structures is not thermally activated. The frequency of electron hoping between Fe^{2+} and Fe^{3+} ions is used to explain the variations in dielectric constant with temperature. The local displacement in the direction of electric field caused by electron hopping is considered as the main cause for increase in dielectric constant which in turn leads to dielectric polarisation in ferrite phase [28].

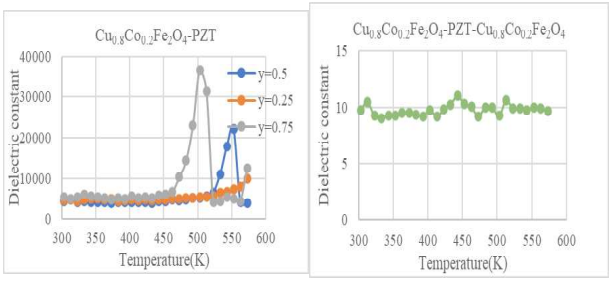


Figure 6 : Variation of dielectric constant with temperature for particulate ME composite $yCu_{0.8}Co_{0.2}Fe_2O_4$-(1-y)PZT and laminated tri-layered thick films ($Cu_{0.8}Co_{0.2}Fe_2O_4$/PZT/ $Cu_{0.8}Co_{0.2}Fe_2O_4$) at 1kHz.

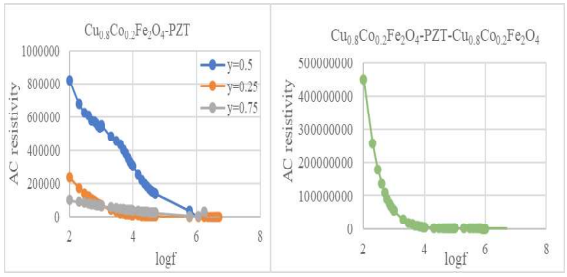


Figure 7 : Variation of AC resistivity with frequency for particulate ME composite $yCu_{0.8}Co_{0.2}Fe_2O_4$-(1-y)PZT and laminated tri-layered thick films ($Cu_{0.8}Co_{0.2}Fe_2O_4$/PZT/ $Cu_{0.8}Co_{0.2}Fe_2O_4$) measured at room temperature.

Figure 7 depicts AC resistivity measurements with frequency for both composites. According to the figure, for particulate composites of $yCu_{0.8}Co_{0.2}Fe_2O_4$-(1-y)PZT with y=0.25,0.5,0.75, AC resistivity decreases with increasing frequency up to 1MHz and remains constant beyond that frequency. However, for laminated thick films of $Cu_{0.8}Co_{0.2}Fe_2O_4$/PZT/ $Cu_{0.8}Co_{0.2}Fe_2O_4$, as frequency increases, AC resistivity decreases up to around 10kHz and then reaches saturation. The variation in AC resistivity with frequency is caused by charge carriers hopping from one equivalent ionic site to another [29]. Figure 8 illustrates study of DC

resistivity measurements with temperature for laminated thick film composites as well as particulate composites. For particulate composites, it has been found that DC resistivity decreases as temperature rises and the slope start to change at a temperature of about 400 K. The obtained DC resistivity measurements for particulate composites show a similar trend to that of the laminated thick films. The DC resistivity graph with temperature is found to obey the Arrhenius equation, which is given by

$$\rho=\rho_0 \exp(\Delta E/KT)$$

where K is the Boltzmann constant, ρ_0 is the temperature-independent constant, ΔE is the activation energy and ρ is the resistivity at temperature. DC resistivity measurement provides information about the semiconducting nature of the samples with conduction occurring primarily due to impurities at low temperatures and the polaron hopping mechanism at high temperatures [30].

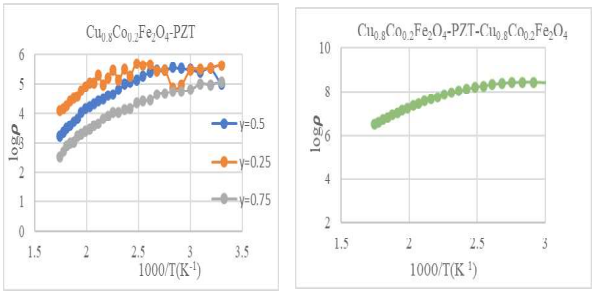


Figure 8: Variation of DC resistivity with temperature for particulate ME composite $yCu_{0.8}Co_{0.2}Fe_2O_4$-(1-y)PZT and laminated tri-layered thick films ($Cu_{0.8}Co_{0.2}Fe_2O_4$/ PZT/ $Cu_{0.8}Co_{0.2}Fe_2O_4$) measured at room temperature.

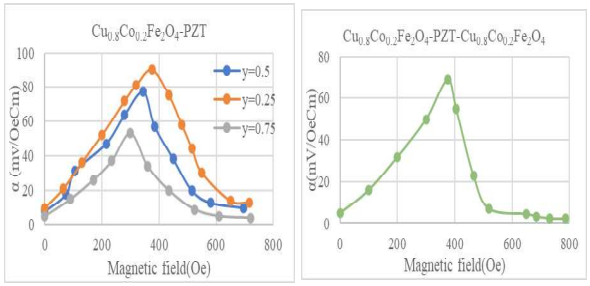


Figure 9: Variation of ME coefficient with magnetic field for particulate ME composite $yCu_{0.8}Co_{0.2}Fe_2O_4$-(1-y)PZT and laminated tri-layered thick films ($Cu_{0.8}Co_{0.2}Fe_2O_4$/ PZT/$Cu_{0.8}Co_{0.2}Fe_2O_4$)

Figure 9 depicts the variation of the transverse magnetoelectric (ME) coefficient with respect to varying applied DC magnetic field. The ME coefficient gradually increases with increasing applied DC magnetic field for both composites, reaching a peak value at one applied field and then decreasing further with increasing field. The growth and orientation of domains in the piezomagnetic phase increase as the applied DC magnetic field increases reaching a peak value at some applied magnetic field and then start decreasing. As a result, a peak is observed in the curves of all samples, indicating that domain growth and orientation are at their maximum resulting in maximum magnetostriction and consequently maximum ME coefficient [31]. The resistivity of composite materials is an important parameter that influences the ME coefficient values. Even though charge leakage is minimised as resistivity increases, ME coefficient values increases. Peak ME coefficients for particulate samples are obtained at around 90 mv/OeCm, 77 mv/OeCm, and 53 mv/ OeCm for y=0.25,0.5,0.75 composites in the applied DC magnetic field range of 375Oe, 320Oe and 300Oe respectively. However, for laminated thick film composites peak ME coefficients are obtained at about 69 mv/OeCm in applied DC magnetic field of around 375Oe respectively.

4. Conclusions

By using the solid-state reaction method, magnetoelectric composites with the ferrite phase $Cu_{0.8}Co_{0.2}Fe_2O_4$ and ferroelectric phase PZT are created. Individual ferrite phases with cubic spinel structures and ferroelectric phases with tetragonal perovskite structures are analyzed using X-ray characterization. The dielectric constant of particulate composites decreases rapidly with increasing frequency and reaches saturation at higher frequencies, with dielectric constants of about 1060, 61.4 and 536 observed at low frequency for y= 0.25, 0.5, and 0.75 respectively. The dielectric constant of laminated thick film composites decreases up to 1MHz and increases above that frequency, with a low-frequency dielectric constant of around 3.35. Loss tangent for particulate composites exhibits a frequency dependence similar to that of dielectric constant with frequency and is found to be 3.29, 3.7and 0.71 for y= 0.25, 0.5 and 0.75 respectively. The loss tangent of laminated film composites of

$Cu_{0.8}Co_{0.2}Fe_2O_4$/PZT/$Cu_{0.8}Co_{0.2}Fe_2O_4$ decreases slightly up to 1KHz and increases slightly above that frequency and is found to be 0.11 at low frequency. With the exception of y=0.25 composites, variation of dielectric constant with temperature exhibits absorption peaks at 553K and 503K for y=0.5 and 0.75 respectively which correspond to Curie temperature. Dielectric constant for laminated thick films is constant up to 400^0 K and increases with temperature above that point. Furthermore, since electron hopping is not thermally activated in these structures, dielectric constant is flat below 400^0 K. AC resistivity decreases with increasing frequency up to 1MHz for particulate composites of y$Cu_{0.8}Co_{0.2}Fe_2O_4$-(1-y)PZT with y=0.25,0.5,0.75 and remains constant beyond that frequency. However, as frequency increases for laminated thick films of $Cu_{0.8}Co_{0.2}Fe_2O_4$/PZT/ $Cu_{0.8}Co_{0.2}Fe_2O_4$, AC resistivity decreases up to around 10kHz and then reaches saturation. It has been observed that for particulate composites, DC resistivity decreases as temperature rises and the slope begins to change around 400 K. The measured DC resistivity of particulate composites follows a similar pattern to that of laminated thick films. The DC resistivity graph with temperature obeys the Arrhenius equation. For both composites, ME coefficient gradually increases with increasing applied DC magnetic field peaking at one applied field and then decreases further with increasing field. Peak ME coefficients are obtained for particulate samples at about 90 mV/OeCm, 77 mV/OeCm, and 53 mV/OeCm for y=0.25, 0.5, and 0.75 composites in the applied DC magnetic field range of 375 Oe, 320 Oe, and 300 Oe, respectively. For laminated thick film composites, peak ME coefficients are obtained at approximately 69 mV/OeCm in a DC magnetic field of 375Oe respectively.

Acknowledgments

The authors are thankful to Dr. G. Ram Gopal, Principal, Dr. G. Sriprakash, HoD and Dr. N. Hanumanth Raju, Department of Physics, Maharani Cluster University, Bangalore for their continuous support during this research work.

Reference

[1] Manish Kumar, S. Shankar, Arvind Kumar, Avneesh Anshul, M. Jayasimhadri et.al 2020, Journal *of Materials Science: Materials in Electronics* **31** 19487.

[2] Deepak Rajaram Patil, Ajeet Kumar, and Jungho Ryu 2021, *Sensors (Basel)* **21** 8012.

[3] Shuai Dong, Hongjun Xiang, Elbio Dagotto 2019*, National Science Review* **6** 629.

[4] Nan CW, Bichurin MI, Dong SX et al 2008, *J Appl Phys* **103** 031101.

[5] Dhiren K. Pradhan, Shalini Kumari and Philip D. Rack 2020, *Nanomaterials* **10** 2072.

[6] Liliana Mitoseriu 2005, *Bol. Soc. Esp. Ceram. V.,* **44** 177.

[7] Shivangi Tiwari and Satish Vitta 2018, *Sci Rep*. **8** 11619.

[8] Shaoyi Xu, Qiang Peng, Chuansheng Li , Bo Liang , Junwen Sun et.al 2021, Appl. Sci. **11** 161.

[9] Jia-Mian Hu and Ce-Wen Nan 2019, *APL Materials* **7** 080905.

[10] L.E. Fuentes-Cobas,J.A. Matutes-Aquino,M.E. Botello-Zubiate,A. Gonza´lez-Va´zquez et.al 2015, *Handbook of Magnetic Materials* **24** 237.

[11] G. Hassnain Jaffari, Junaid Ur Rehman, LayiqZia 2020, *Materials Chemistry and Physics* **245** 122757.

[12] S. D. Chavan, S. G. Chavan, S. S. Mane et.al 2016 *Journal of Materials Science: Materials in Electronics* **27** 1254.

[13] Shivangi Tiwari and Satish Vitta 2018, *Scientific Reports* **8** 11619.

[14] Rahul Goel, Rajat Syal, Gyaneshwar Sharma, Ramesh Kumar Singh et.al 2022, *Materials Chemistry and Physics* **282** 126004.

[15] John Paul Praveen, Monaji Vinitha Reddy, Jayant Kolte, Sakthivel Dinesh Kumar et.al 2016, *Int J Appl Ceram Technol* **14** 200.

[16] Dipti, J. K. Juneja, Sangeeta Singh, K. K. Raina 2015, *Ferroelectrics Letters Section* **42** 97.

[17] R.Grigalaitis, M.M.Vijatović ,Petrović , J.D.Bobić 2014, *Ceramics International* **40** 6165.

[18] Aleksandr A.Naberezhnov, Ivan A.Dolgakov, Mikhael Tovar 2016, *St. Petersburg Polytechnical University Journal: Physics and Mathematics* **2** 181.

[19] Shuxiang Donga, Junyi Zhai, Naigang Wang, Feiming Bai, JieFang Li, and D. Viehland 2015, *Appl. Phys. Lett.* **87** 222504.

[20] A. S. Karapuzha, N. K. James, H. Khanbareh, S. van der Zwaag and W. A. Groen 2016, *Ferroelectrics* **504** 160.

[21] Vijendra A Chaudhari, Govind K Bichile 2010, *Physica B* **405** 534.

[22] S.P. Yadav, S.A. Kanade, Kamlesh V. Chandekar 2021, *International Journal of Aquatic Science* **12** 2554.

[23] D M Jnaneshwara, D N Avadhani, Daruka Prasad B, NagaBhushana 2014, *Spectrochimica Acta Part A Molecular and Biomolecular Spectroscopy* **132C** 256.

[24] G. H. Jonker 1959, *Journal of Physics and Chemistry of Solids* **9** 165.

[25] M Azizar Rahman and A K M Akther Hossain 2014, *Phys. Scr.* **89** 115811.

[26] Amira Bougoffa, E. M. Benali, A. Benali, M. Bejar, E. Dhahri, M. P. F. Graça, M. A. Valente, G. Otero-Irurueta, and B. F. O. Costa 2022, *RSC Adv.***12** 6907.

[27] L. R. Naik and B. K. Bammannavar 2011, *Ferroelectrics* **14** 265.

[28] Shubhra Mathur, Subodh Srivastava, Sachin Surve, Kiran Wadhwani et.al 2017, *Mater. Res. Express* **4** 126101.

[29] Dhiren K. Pradhan, Shalini Kumari, Venkata S. Puli, Proloy T. Das 2017, *Phys. Chem. Chem. Phys.***19** 210.

[30] S.U. Durgadsimi, S.S. Chougule et.al 2011, *International Journal of Engineering Science and Technology* **3** 1446.

[31] Pietro Galizia, Carlo Baldisserri, Elisa Mercadelli, Claudio Capiani, Carmen Galassi and Miguel Algueró 2020, *Materials (Basel).* **13** 2592.